The 7th World Congress on Particle Technology (WCPT7)

Numerical Modelling of ESP for Design Optimization

Baoyu Guo[a*], Aibing Yu[a], and Jun Guo[b]

[a]*Lab for Simulation and Modelling of Particulate Systems, School of Materials Science and Engineering,
University of New South Wales, Sydney, 2052, Australia*
[b]*Experimental and Research Centre, Fujian Longking Co., Ltd., Longyan, 364000, China*

Abstract

Electrostatic precipitators (ESP) are widely used for collection of particulate matters. In the present paper, a Computational Fluid Dynamics (CFD) model, based on Eulerian-Lagrangian framework, is used to simulate the gas-particle flow under electric field. A typical two-stage ESP is chosen as a case study and its collection performance is assessed under a series of modified geometric conditions, including inlet pipework, perforated plate, addition of flow baffles, and spatial extent of electric field. The results show that the collection efficiency for PM2.5 can be increased by 20% after optimization.

Keywords: Particle Flow; Electrostatic Precipitator (ESP); Numerical Modeling

1. Introduction

Electrostatic precipitators (ESP) are widely used in coal-fired power generation plants for removing fine particulate matter. ESPs prove to have a high mass efficiency and the advantages of large handling capacity with low pressure loss. However, the major problems arise from the increasing demand for collection efficiency of fine particles (e.g., PM2.5) and further requirement on device optimization.

An industrial ESP is not only structurally complicated, as shown in Figure 1, but also involves complicated transport phenomena, including electric field, gas-particle flow, and strong interactions among them. Firstly the corona is generated at the small needle tip of the emitter electrode, which controls the distribution of the electric

---

* Corresponding author. E-mail address: baoyu@unsw.edu.au

field intensity and ion charge in the collection passage [1]. Then non-uniform electric current induces ionic wind that affects the turbulence level and particle diffusion and re-entrainment [2,3]. Particles are charged and driven to the collection plates to build up cake layers. Numerical simulations of these processes are becoming popular, but most of them so far have focused largely on the local corona region or specific phenomena [4-6]. A full scale ESP prediction tool with all these key phenomena considered together is rare. To date, in the ESP design, engineers still rely on the over-simplified Deutsch equation [7]. Following the earlier development of an integrated model to describe the major transport phenomena [8], the current paper will further investigate the model applicability in the design optimization of wire-plate type ESP.

Nomenclature

b	ion mobility
d_p	diameter of particle
Cc	Cunningham correction factor
C_D	drag coefficient
D	ionic diffusivity
E	E-field intensity
F	force
g	gravitational acceleration
k	turbulent kinetic energy
k_0	Boltzmann constant
m_p	mass of a particle
P	pressure
q	particle charge
q_e	unit electron charge
T	temperature
t	time
U,u	velocity
V	electric potential
ρ	density
μ	gas dynamic viscosity
μ_t	eddy viscosity
ω	turbulence eddy frequency
ε_0	electric permittivity
ρ_{ion}	ion space charge density
κ_p	dialectic constant of particles

2. Method

The model is developed based on the framework of ANSYS-CFX (release 14), combined with user subroutines. The Poison equation of potential and current continuity equation are solved for the electric field and space charge density. The Eulerian-Lagrangian method is used for the gas-particle flow. The k-ω based Shear Stress Transport (SST) model is chosen for turbulence. The major governing equations are given below.

Electric field

$$\nabla^2 V = -\rho_{ion} / \varepsilon_0 \tag{1}$$

$$\nabla \bullet (\, \rho_{ion} b \mathbf{E}) - D\nabla \rho_{ion}) = 0 \tag{2}$$

$$\mathbf{E} = -\nabla V \tag{3}$$

Gas flow

$$\nabla \cdot (\rho \mathbf{U}) = 0 \tag{4}$$

$$\nabla \cdot (\rho \mathbf{U} \otimes \mathbf{U}) = \nabla \cdot (P + \tfrac{2}{3}\rho k) + \nabla \cdot [(\mu + \mu_t)(\nabla \mathbf{U} + (\nabla \mathbf{U})^{\mathrm{T}})] + \mathbf{F}_{EHD} \tag{5}$$

$$\mu_t = \rho \frac{a_1 k}{\max(a_1 \omega, SF_2)} \tag{6}$$

Particle flow

$$m_p \frac{d\mathbf{u}_p}{dt} = \frac{1}{8} C_D \pi d_p^2 \rho_f \mid \mathbf{u}_f - \mathbf{u}_p \mid (\mathbf{u}_f - \mathbf{u}_p) + \frac{1}{6}\pi d_p^3 \mathbf{g}(\rho_p - \rho_f) + q\mathbf{E} + \mathbf{F}_{dis} \tag{7}$$

Particle charging rate [9]

$$\frac{dv}{d\tau_q} = \begin{cases} f(w)\dfrac{v - 3w}{\exp(v - 3w) - 1}, & v > 3w \\[2mm] \dfrac{3w}{4}\left(1 - \dfrac{v}{3w}\right)^2 + f(w), & -3w \le v \le 3w \\[2mm] -v + f(w)\dfrac{-v - 3w}{\exp(-v - 3w) - 1}, & v < -3w \end{cases} \tag{8}$$

where $v = \dfrac{qq_e}{2\pi\varepsilon_0 d_p k_0 T}, w = \dfrac{\kappa_p}{\kappa_p + 2}\dfrac{Ed_p q_e}{2k_0 T}, \tau_q = \dfrac{b\rho_{ion} t}{\varepsilon_0}, f(w) = \min(1, (w + 0.475)^{-0.575})$

Electro-hydra dynamic (EHD) secondary flow (or ionic wind) is treated as additional turbulence productions, which are added in the turbulence equations as sources. This treatment effectively accounts for the enhanced global mixing of gas flow, and thus affects the overall flow pattern to some degree, without considering the detailed local flow structures. This, however, has an implication for the particle flow modelling. For particle flow, the eddy interaction model with random walk method is used outside the electric field [10]. In the electric field, the turbulent dispersion force is switched off in the present study, for the following reason: the EHD flow in the ESP is believed to adversely affect the overall collection efficiency [11,12]. When the EHD flow is treated as turbulence from macroscopic viewpoint, diffusion of suspended particle will be promoted and subsequently the wall collision frequency will be dramatically increased, which will lead to over-prediction of the collection efficiency. This is contradictory to the general knowledge of EHD effect as mentioned above. Nevertheless, without resolving the detailed local particle characteristics, the current hybrid treatment appears to give statistically sensible predictions of the overall particle collection efficiency, which should be sufficient for the purpose of design optimization based on comparative studies.

3. Result and discussion

3.1. Conditions

A two-stage ESP model is shown in Fig.1. Two perforated plates with porosity f = 0.5, 0.4 respectively are used in the diffuser. Ten vertical vanes are attached to the perforated plates on the back side. The rectangular chamber (6m long, 1.25m wide, 2.2m high) includes two electric fields (first and second electric field) in series separated by a middle way barrier in the lower part. 64 barbed wire electrodes of 8mm in diameter are restricted to a narrow region in height. Four hoppers are at the bottom with partition plates in the first and the last ones. Geometric symmetry allows only one half of the ESP to be considered. The gas flow rate is specified at the inlet such that the mean velocity in the collection field is about 1.0 m/s.
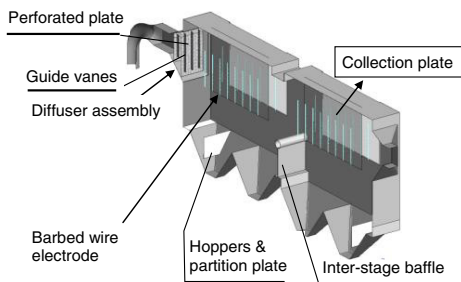

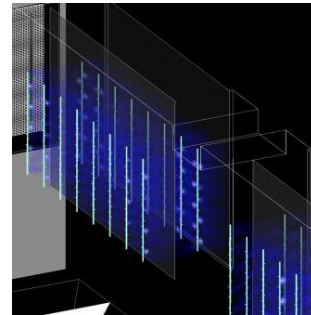Fig.1. Model geometry for a two-stage ESP

Fig.2. Rendered space charge density distribution.

3.2. Typical result for base case

Electric field and space ion charge density are solved locally in a unit cell model around a single barb on the wire [13]. The field distribution obtained is then implemented in the ESP model via a modular approach using periodical symmetry conditions (as visualized in Fig.2).

Very complicated flow pattern is found in the collection chamber (Fig.3). The particles tend to go downwards after exiting the diffuser. The reasons are a), top wall and the bottom wall have different slope angles (30° and 45° respectively); b), a large free space exists at the lower part of the chamber; c), the pipe bend and transition of the cross section in the inlet pipe work adversely affect the flow uniformity to the diffuser. The simulation shows a large size recirculation in the first electric field. A small portion of particles may fluctuate to the top above the electric region, whereas most of the particles go downward around the recirculation eddy, and then turn around upwards before entering the second stage chamber. These particles have little chances of being charged in the 1st electric field.
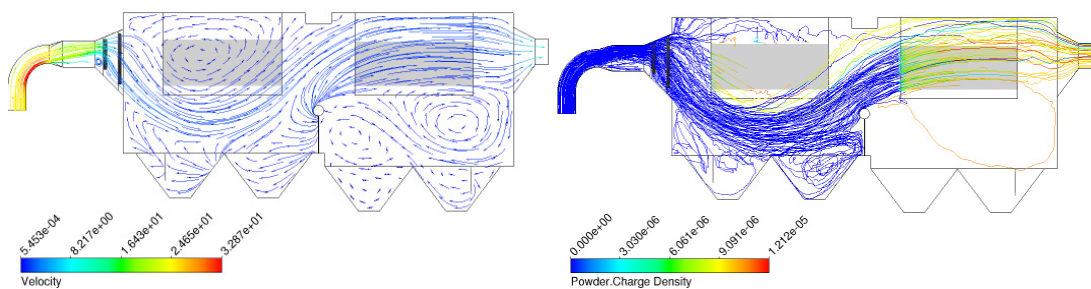

Fig.3. Gas flow streamlines on the symmetry plane and particle trajectories for the base case.

Fig.4 shows the collection efficiency on the collection plates for different particle sizes. A theoretical analysis of particle charging capacity and force balance between the drag and electric force on a single particle indicates that the settling velocity is inversely proportional to the particle size. Therefore, the collection efficiency is expected to increase with the particle size in all the cases. However, the rate of change with respect to the particle size varies for different particle sizes. For ultra-fine particles, the efficiency increases slowly due to a smaller charging rate. It is also noted that the collection efficiency gradually approaches a higher limit when particle size increases beyond 4μm. In this case, the particles have escaped largely via the by-passing flow.
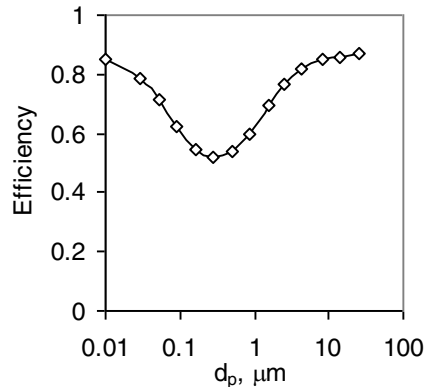

Fig.4. Collection efficiency as a function of particle size (Case B).

3.3. Case studies

Since PM2.5 is of practical concern, the collection efficiency for particle size of d_p = 2.5μm is predicted in this section. The cases considered involve the following modifications: inlet pipe, baffles, perforated plate parameters and electric field position& extent. Reasons for the emissions can be diagnosed by showing the trajectories of the emitted particles that exit the system through the outlet (Fig.5). The color is scaled to the particle surface charge density in unit $[As/m^2]$.

For the original design, Case A, the particles after the diffuser spread widely in space. Nearly all the particles that enter the 1st electric field, despite small in number, are successfully collected. The collection rate on the plate is highly uneven and localized, with large portion of the collection area being wasted Fig.6(a). It is the large recirculating eddy that prevents particles from entering the electric field directly. Collection occurs mainly in Stage-2. For the particles that exit the outlet, the electric charge on the particles is low in average (7.4e-3 [As/kg]), and also varies widely, which indicates inadequate and uneven particle charging conditions. Due to highly localized space charge density, free ion charges never appear over certain space (e.g., in the close proximity of the wire surface for the barbed wire electrode) in the electric field. Therefore, a small number of particles may happen to pass these so-called "dead zones" without being charged.

In Case B, the inlet pipe is replaced by a straight square duct. This eliminates the eddy behind the original transition part, so that the inlet velocity profile to the diffuser becomes almost uniform. As a consequence, the downward momentum after the diffuser is reduced, directing more particles to the 1st electric field. The collection rate is increased by 74% in the first stage and the total efficiency is up by 10 percentage points.

In the previous cases, many particles after the diffuser are moving into upper and lower parts in the first stage chamber. This can be improved in Case C, by adding a flow baffle underneath and blocking a part of 2nd perforated plate at the top margin (0.1m). This modification significantly reduces the by-pass particle flow, thus increasing the collection efficiency from 76.7% to 83.7%. However, since the velocity in the first electric field increases, not all the particles have sufficient residence time to charge to their full capacity and to deposit in the 1st stage. These failed particles retain the charges obtained and proceed into the second stage.

In Case C, the charged particles that have escaped from 1st stage tend to concentrate at the upper edge of the 2nd electric field. This can be improved by up-shifting the 2nd stage electric field, or alternatively (i.e., Case D), extending the 2nd electric field up by 0.225m (or the distance of three needles). Then the total collection efficiency can be increased from 83.7% up to 91.6%, although at the sacrifice of extra power consumption. The average charge carried by the escaped particles is 0.011 [As/kg] compared with 7.4e-3 [As/kg] in the base case. In addition, nearly all the particles have been highly charged with small deviation. These suggest that the particles charging conditions have improved. Moreover, the deposited dust layer covers plates in all the electric field with less bias Fig.6(b). However, many particles manage to escape via a free space above the second electric field in Case D, so local modifications in this region may help the collections even further.

To summarize, the original inlet pipe assembly (pipe bend, transition section) in place of a straight square duct has negative effect. A solid plate margin (to block the orifices) at the top of the second perforated plate can reduce the by-passing above the electric field. Without baffles, most particles tend to deposit in Stage-2 in stead of Stage-1. Adding a single baffle is able to reverse this trend. Adjusting the position and/or extent of the electric field region in stage-2 can improve the total collection efficiency.

Table 1. Collection efficiency of different parts.

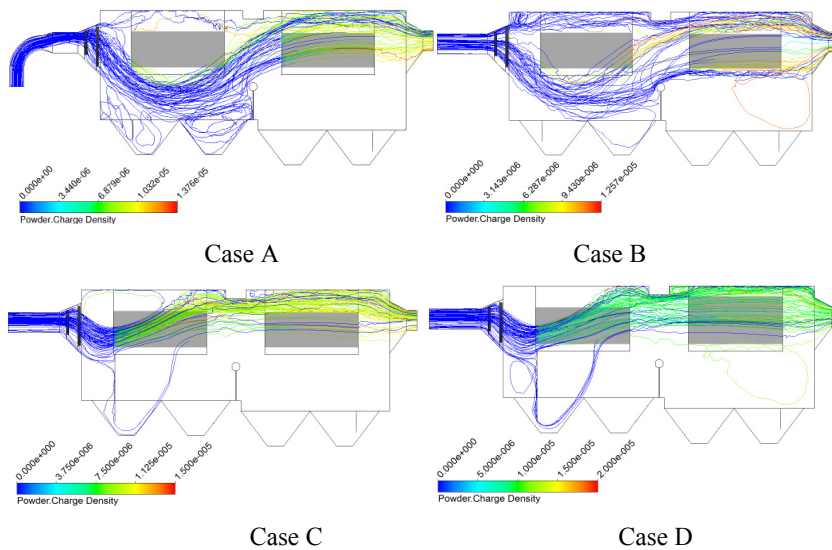| Case	Stage-1	Stage-2	Hoppers	Total
A	18.9	46.2	1.4	66.7%
B	32.9	41.1	2.6	76.7%
C	58.7	23.7	1.4	83.7%.
D	58.5	31.4	1.4	91.6%

Fig.5. Trajectories of escaping particles in the ESP before and after modification.
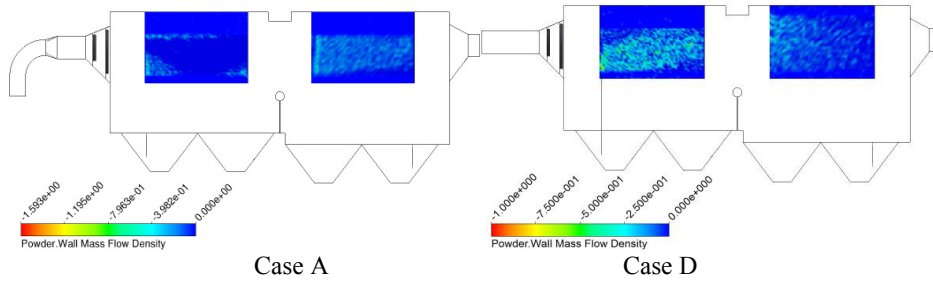
Fig.6. Pattern of particle deposition on the collection plates before and after modification.

4. Conclusion

A CFD model is presented for the simulation of the gas-particle flow in an industrial ESP. Particularly the collection performances for fine particles are examined in several cases. For the original design, a large-scale eddy is found in the first-stage collection region, which turns the particles away and causes a waste of space and electric power. It is demonstrated that proper modifications can regulate the turbulent gas flow pattern, and subsequently the particle behaviors. The predictions show that the particle collection efficiency for PM2.5 can be potentially improved from the original 67% up to 91% after modification. By tracking particle motions, fine particles may escape due to by-pass flow and insufficient particle charging. The numerical experiments provide useful guidance for the ESP unit optimization.

Acknowledgements

References

[1] N.Neimarlija, I.Demirdzic, S.Muzaferija, Finite volume method for calculation of electrostatic fields in electrostatic precipitators, J. Electrostatics 67 (2009) 37-47.

[2] A.Soldati, On the effects of electrohydrodynamic flows and turbulence on aerosol transport and collection in wire-plate electrostatic precipitators, J. Aerosol Science 31(2000) 293-305.

[3] N.Farnoosh, K.Adamiak, G.S.P.Castle, 3D numerical analysis of EHD turbulent flow and mono-disperse charged particle transport and collection in a wire-plate ESP, J. Electrostatics 68 (2010) 513-522.

[4] McLean, K.J. Electrostatic precipitators, IEE Proceedings 135 (A6) (1998) 347-361.

[5] K.S.P.Nikas, A.A.Varonos, G.C.Bergeles, Numerical simulation of the flow and the collection mechanisms inside a laboratory scale electrostatic precipitator, J. Electrostatics 63(2005) 423-443.

[6] N.Farnoosh, K.Adamiak, G.S.P.Castle, Three-dimensional analysis of electrohydrodynamic flow in a spiked electrode-plate electrostatic precipitator, J. Electrostatics 69 (2011) 419-428.

[7] K.R.Parker, Applied Electrostatic Precipitation, Springer, 1997.

[8] B.Y.Guo, S.Y.Yang, M.Xing, K.J.Dong, A.B.Yu, J.Guo, Towards the development of an integrated ESP model, I&ECR 52 (2013) 11282-11293

[9] P.A.Lawless, Particle charging bounds, symmetry relations, and an analytic charging rate model for the continuum regime, J. Aerosol Sci. 27(1996) 191-215.

[10] A.D.Gosman, E.Ioannides, Aspects of computer simulation of liquid-fuelled combustors. J. Energy 7(1983) 482−490.

[11] A.Soldati, On the effects of electrohydrodynamic flows and turbulence on aerosol transport and collection in wire-plate electrostatic precipitators, J. Aerosol Sci. 31(2000) 293-305.

[12] K.S.P.Nikas, A.A.Varonos, G.C.Bergeles, Numerical simulation of the flow and the collection mechanisms inside a laboratory scale electrostatic precipitator, J. Electrostatics 63(2005) 423-443.

[13] B.Y.Guo, J.Guo, A.B.Yu, Simulation of the electric field in wire-plate type electrostatic precipitators, J. Electrostatics, 2014, (submitted)